Rock Dynamics – Experiments, Theories and Applications – Li, Li & Zhang (Eds)
© 2018 Taylor & Francis Group, London, ISBN 978-0-8153-9667-3

Validation of a mathematical model for evaluating the dynamic shear strength of rock

T. Okada
Central Research Institute of Electric Power Industry, Chiba, Japan

T. Naya
Dia Cosultants Co. Ltd., Saitama, Japan

ABSTRACT: The purpose of this research is to verify our proposed mathematical model for estimating the dynamic shear strength of rocks and to establish an evaluation procedure for obtaining dynamic shear strength. Monotonic loading tests and cyclic loading tests of natural tuff were conducted to obtain the mathematical model parameters. Then multistep shear tests under cyclic and seismic-wave loadings were performed, followed by simulations using the mathematical model. The test results showed the dynamic strength exceeding the static strength, agreeing with previous research. Furthermore, the dynamic strength calculated from the mathematical model of natural tuff was generally consistent with the dynamic strength obtained from the experimental data.

1 INTRODUCTION

Revisions to seismic design review guidelines for nuclear power plant facilities have increased the level of seismic ground motion designs from the level of traditional designs, thereby increasing the importance of dynamic analysis when evaluating the stability of the power plant's foundation bedrock and the rock slope around it. This has also increased the need to correctly evaluate the physical properties of the bedrock used in dynamic analyses, particularly dynamic strength. Dynamic strength, which is the strength used in dynamic analyses, does not have a clear definition, but for purposes of seismic design it can be said to be the strength exerted when a cyclic shear stress is applied in an irregular waveform such as a seismic wave. Because seismic waveforms are diverse, and the stress (waveform) inside the ground also varies depending on the location, it is difficult to formulate a single definition of dynamic strength. For these reasons, in current usage, the strength exerted when a sinusoidal load is applied is generally called the "dynamic strength."

In the seismic design of nuclear power plants, static strength has traditionally been used, based on the fact that when comparing dynamic and static strengths, the dynamic strength does not fall below the static strength (JEA 2008). This "dynamic strength $\geq$ static strength" relationship has been confirmed for various rock types (Nishi & Esashi 1982, Yoshinaka et al.1987, Sugiyama et al. 2001, Ookuma 2010, Okada and Ito 2009). However, this data is mostly from pulsating loading in which the direction of shear stress is not reversed and includes no alternating loading data. In addition, there is considerable data for incremental loading of sinusoidal waves and much less data for seismic (irregular) waves, and the relationship between the two is not clear. To resolve these issues, in this research, in addition to comparing pulsating loading to alternating loading using natural tuff, we conducted multistep cyclic loading tests using sine waves and seismic waves. Finally, we validated our proposed mathematical model for evaluating dynamic strength by comparing it with the test results.

2 MATHEMATICAL MODEL OUTLINE OF DYNAMIC STRENGTH

2.1 *Effect of fatigue*

When the stress amplitude is fixed and repeated stress is applied until the failure of specimen, the stress amplitude decreases as the number of cycles increases. The function expressing this relationship is defined as the fatigue function f_1 and expressed as follows:

$$f_1(N_f) := \frac{\tau_{f\_N_f}}{\tau_{f\_N=1}} = 1 - a \cdot \log N_f \tag{1}$$

where N_f ($\geqq 1$) is the number of cycles at the time of failure, τ_{f_Nf} is the shear strength at the time of failure after the loading N_f, $\tau_{f\_N=1}$ is the shear strength during monotonic loading, and a is a parameter defining the slope of the function, which means that the decrease in strength is greater for larger values of a.

2.2 *Effect of loading rate*

It is also known that strength tends to increase as the loading rate increases. In contrast to the fatigue effect, which always decreases the strength as the number of repetitions increases, increasing the loading rate tends to increase the strength. In our proposed mathematical model, the relationship between dynamic and static strengths is determined mainly by these two effects. We define the function f_2 as the function that represents the relationship between the loading rate and shear strength, and define it as follows:

$$f_2(\dot{\varepsilon}) := \tau_f = \alpha + \beta \cdot \log \dot{\varepsilon} \tag{2}$$

where $\dot{\varepsilon}$ is the axial strain rate (%/min), τ_f is the maximum shear strength (MPa), and α and β are parameters.

2.3 *Integration of fatigue and loading rate effects*

Letting τ_f in Eq. (2) be the strength $\tau_{f\_N=1}$ at loading time N = 1 in Eq. (1), the following relationship is obtained:

$$\tau_{f\_N_f} = f_1 \cdot f_2 = (\alpha + \beta \cdot \log \dot{\varepsilon})(1 - a \cdot \log N_f) \tag{3}$$

From this, the relationship between N_f ($\geqq 1$) and τ_{f_Nf} at any strain rate can be obtained. Note that the derivation of Eq. (3) assumes that the relation in Eq. (1) is satisfied regardless of the loading rate. However, experimental data confirms that this assumption is to some extent reasonable (Okada & Ito 2009).

2.4 *Application of cumulative damage rule*

To express the impact of an arbitrary waveform in the mathematical model, it is necessary to know the impact of the cyclic loading that leads to fracture (hereinafter referred to as the "damage effect"). However, because no such test data was available, we applied the cumulative damage rule used in metal materials design (Otaki 2007). The strength exerted after N wave loading (hereinafter referred to as "residual strength") is assumed to change linearly with respect to its fracture count. Adopting this perspective, the damage function f_3 representing the effect of damage due to cyclic loading can be expressed as follows:

$$f_3(N) := \frac{\tau_{d\_N}}{\tau_{f\_N=1}} = 1 - d \cdot (N - 1) \tag{4}$$

where N is the number of cycles on the way to failure, and τ_{d_N} is the strength (residual strength) exerted after N cycles. At the time of failure (when $N = N_f$), Eq. (1) = Eq. (4) obtains. Because $f_1(N_f) = f_3(N_f)$, the following relation is obtained:

$$d = \frac{a \cdot \log N_f}{N_f - 1} = \frac{1 - \dfrac{\tau_{f\_N_f}}{\tau_{f\_N=1}}}{10^{\frac{1 - \frac{\tau_{f\_N_f}}{\tau_{f\_N=1}}}{a}} - 1} \tag{5}$$

Therefore, the parameter d in Eq. (4) is determined from Eq. (5) when the stress ratio $\frac{\tau_{f\_N_f}}{\tau_{f\_N=1}}$ is determined. The following relationship is then obtained from Eqs. (2) and (4):

$$\tau_{f\_N_f} = f_2 \cdot f_3 = (\alpha + \beta \log \dot{\varepsilon})\{1 - d(N-1)\} \tag{6}$$

Note that for Eq. (6) to hold in the same way as Eq. (3), the relationship shown in Eq. (4) must hold regardless of the loading rate. Lacking empirical data on this issue, here we make the same assumptions as the cumulative damage rule. This assumption makes it possible to determine the degree of damage even if the stress ratio $\frac{\tau_{f\_N_f}}{\tau_{f\_N=1}}$ is determined at different loading rates.

2.5 *An example of dynamic strength calculation*

Figure 1 shows an example of calculating the dynamic strength when different stress amplitudes are applied. Loading is performed 6 times at stress ratio 0.9, 30 times at stress ratio 0.8, and 600 times at stress ratio 0.7. As shown in the figure, when cyclic loading is applied five times at a stress ratio of 0.9, the vertical axis (residual strength) is 0.94. Next, when cyclic loading is applied continuously at a stress ratio of 0.8, the residual strength of 0.94 carries over (it moves to the right in the figure), and the damage at the 0.8 stress ratio is the same as for the previous 30 iterations. When loading is iterated a further 30 times from this point, the residual strength becomes 0.88. When cyclic loading is again applied continuously at stress ratio 0.7, the residual strength of 0.88 is carried over (moves further to the right in the figure), and the damage at stress ratio 0.7 is the same as for the previous 400

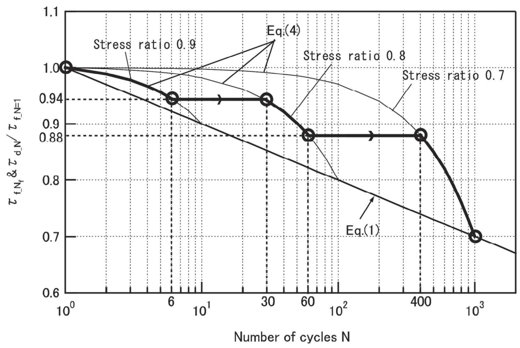

Figure 1. Example of calculating dynamic strength using the mathematical model.

iterations. After cyclic loading is applied another 600 times from this point, the residual strength reaches 1000 cycles expressed in Eq. (1), which means failure occurs.

Dynamic strength can therefore be defined as the strength at the point in time when Eq. (4) matches Eq. (1) (as described above). Note that if the loading rate changes at some point before failure, $\tau_{f\_N=1}$ will change based on Eq. (2). In other words, Fig. 1 would show only a relative change in the stress ratio $\frac{\tau_{f\_N_f}}{\tau_{f\_N=1}}$.

2.6 *Overview of the dynamic strength evaluation method*

Using our proposed mathematical model, the dynamic strength can be obtained by following the steps below.

1. Perform cyclic loading tests at different shear stress amplitudes. The shear stress amplitude is not incremented stepwise in a single test, but is held constant until fracture in only one step.
2. Letting the horizontal axis be the number of iterations (logarithmic) and the vertical axis be the normalized stress ratio, obtain the fatigue function f_1.
3. Perform monotonic loading test at several loading rates in different orders. Set the range of loading rates so that it covers the loading rate in (1) and the static test rates.
4. Letting the horizontal axis be the strain rate (logarithmic) and the vertical axis be the shear strength, obtain the rate function f_2.
5. Using the functions f_1 and f_2 obtained in (2) and (4) above and the damage function f_3, obtain the dynamic strength of various regular waves and irregular waves (seismic waves).

3 VALIDATION OF THE DYNAMIC STRENGTH EVALUATION METHOD

3.1 *Specimens*

The specimens used consisted of rhyolitic welded tuff from the Neogene Miocene (also known as "Oya tuff stone"). Using a core drill, cutter, and edge-shaping machine, block sample specimens (cubes of approximately 30 cm) were shaped into cylindrical specimens of a diameter of approximately 50 mm and a height of approximately 20 mm.

3.2 *Test equipment*

The box shear test equipment used for test. A pneumatic servo-type two-axis loading apparatus is used. Both the maximum vertical load and maximum shear load are 20 kN. A bellofram cylinder is electrically controlled by a pneumatic servo valve, and the load cell output value (voltage) is fed back for control. The specimen is encased in the shear box through steel spacers, and a vertical force is loaded with the pressure plate separated from the shear box. Grease was applied to reduce friction between the pressure plate and the spacer and the shear box.

3.3 *Test method*

All tests were carried out as box shear tests with constant vertical stress. Except for the loading method, the tests confirmed in principle to the constant stress, box shear test method standard (Japanese Geotechnical Society 2009). A list of loading methods and conditions is given in Table 1. Series OT-1 is a monotonic loading test (static test). The strain rate was set to the standard 0.05 mm/min. The vertical pressure was set from 0.2 MPa to 2.0 MPa.

Series OT-2 is a cyclic loading test carried out to investigate the fatigue effect. For comparison, both pulsating and alternating cyclic loading tests were performed. As shown in Figure 2, the maximum shear stress ($2\Delta\tau$) was assumed to be equal under the alternating and pulsating load conditions. In other words, the alternating stress amplitude ($2\Delta\tau$) was twice the pulsating stress amplitude ($\Delta\tau$). Both the loading frequencies were 0.1 Hz, waveforms were sine waves, and the maximum shear stress $2\Delta\tau$ ranged from 1.6 MPa to 2.0 MPa. Note that the vertical pressure was fixed at 0.2 MPa.

Series OT-3, a monotonic loading test for investigating the rate effect, was performed on various strain rates (0.05–10 mm/min).

Series OT-4 is a multistep cyclic loading test for validating the strength evaluation formula. It

Table 1. List of tests.

Series	Purpose	Loading method	Test conditions				Confining pressure (MPa)	Quantity (pcs)
OT-1	Static strength	Monotonic	Strain rate: 0.05 mm/min				0.2 to 2.0	16
OT-2a	Fatigue effect	Cyclic (pulsating)	Frequency: 0.1 Hz, Stress amplitude: 1.6 to 2.0 MPa				0.2	6
OT-2b	Fatigue effect	Cyclic (alternating)	Frequency: 0.1 Hz, Stress amplitude: 1.6 to 2.0 MPa				0.2	7
OT-3	Rate effect	Monotonic loading	Strain rate: 0.05 to 10 mm/min				0.2	8
OT-4a	Model validation	Multistep cyclic	No.	Frequency (Hz)	Waves (times)	Number of steps	0.2	4
			4a-1	1	5	5		
			4a-2	0.1	10	5		
			4a-3	0.01	30	10		
			4a-4	0.5	10	10		
OT-4b	Model validation	Multistep cyclic	No.	Seismic wave		Number of steps	0.2	4
			4b-1	Time axis 50 times		5		
			4b-2	Time axis 20 times		5		
			4b-3	Time axis 10 times		10		
			4b-4	Time axis 5 times		10		

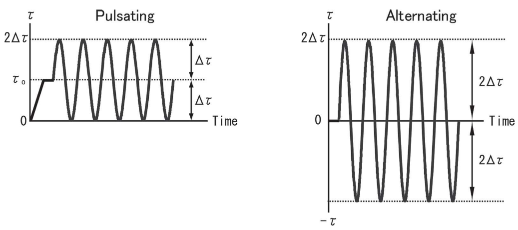

Figure 2. Comparison between pulsating loading and alternating loading.

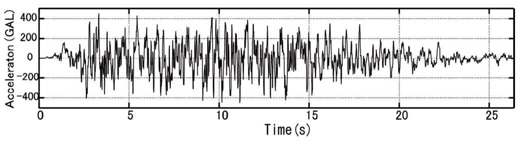

Figure 3. Artificial seismic wave that was used.

is performed entirely using alternating loading. Series OT-4a uses sine waves in the same way as series OT-2a. The frequency, number of waves, and number of steps are as indicated in Table 1. Series OT-4b uses the artificially created seismic wave, indicated in Figure 3 (Nuclear power civil engineering committee ground stability evaluation subcommittee 2004). However, owing to the limitations of the test equipment, as indicated in Table 1, the time axis was set to 5–50 times, and the number of steps to 5–10 steps.

The number of steps n is calculated as follows. Setting the maximum stress amplitude equal to the static strength, the seismic wave causes the stress amplitude at which loading is performed to increase by increments of 1/n at each step until fracture (1/n, 2/n, …, n/n(= static strength), n+1/n, …).

3.4 *Test results and discussion*

The strength characteristics obtained from series OT-1 are shown in Figure 4. The test results exhibit wide variation but yield the values c = 1.38 MPa and ϕ = 51°. Previous triaxial tests on Oya tuff stone under different scales and drainage conditions yielded values of c = 1.5~2.1 MPa and ϕ = 27~35° (Tani 2006). The c value was lower and the ϕ value was higher than the previous research. This can likely be owing to factors like different test methods, different confining pressure levels (smaller stress in our tests), and different miso contents (lower in our tests).

An example of the results of alternating loading in the series OT-2 fatigue test is shown in Figure 5. The shear displacement increases and decreases as the loading progresses, and then shear displacement sharply increases once the shear stress can no longer be maintained (about 76 s). All the test cases show the same clear, rapid increase in shear displacement at specific points. These points were defined as failure points, and were counted and recorded as the number of cycles to failure N_f. Figure 6 shows that the relationship between N_f and the strength normalized with the single-wave fracture strength. This relationship corresponds to Eq. (1). The equation approximated by the least squares method is shown as a solid line in the figure. Although there are fluctuations in the data, no large difference between the pulsating condition and alternating condition can be observed. The parameter values for Eq. (1) were $a = 0.0496$ (pulsating) and 0.0474 (alternating). Compared to the results for natural mudstone ($a = 0.04$~0.1) (Okada & Ito 2009), the fatigue effect was smaller in our tests. Because of the small difference between the pulsating and alternating conditions, the multistep cyclic test (series OT-4) was carried out only under the alternating condition.

The relationship between loading rate and shear strength obtained in the series OT-3 test is shown in Figure 7. Note that the loading rate on the horizontal axis is the shear displacement rate (mm/min). This relationship corresponds to Eq. (2). The equation approximated by the least squares method is indicated by a solid line in the figure. This yields values for the parameters in Eq. (2) of $\alpha = 1.78$, $\beta = 0.158$. Because a represents the strength when the strain rate is 1 mm/min, we divide the right side of Eq. (2) by this value, yielding a value of 0.089 for β/α. This value represents the rate of strength increase due to the increase in strain rate relative to the strain rate of 1 mm/min. This value is larger than the corresponding result for natural mudstone ($\beta/\alpha = 0.07$) (Okada & Ito 2009). Figure 8 shows example results for the multistep cyclic test in series OT-4, both for sine waves (0.1 Hz, 5 steps, 10 waves) and for seismic waves(5 steps, time axis increased 10 times). As the loading progresses, the axial strain increases under both load conditions, and then the axial strain increases when axial differential stress amplitude can no longer be maintained. In all cases the axial strain exhibits the same clear, rapid increase at specific points. These points were defined as failure points, and the maximum stress endured before fracture was defined as the final multistep cyclic

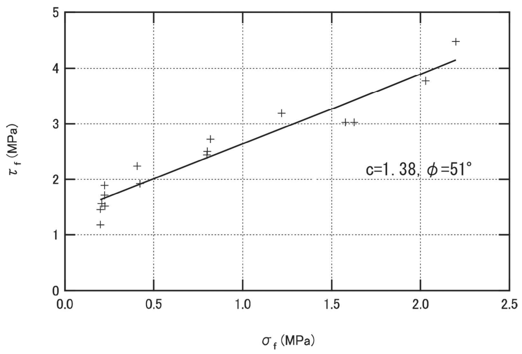

Figure 4. Results of static tests.

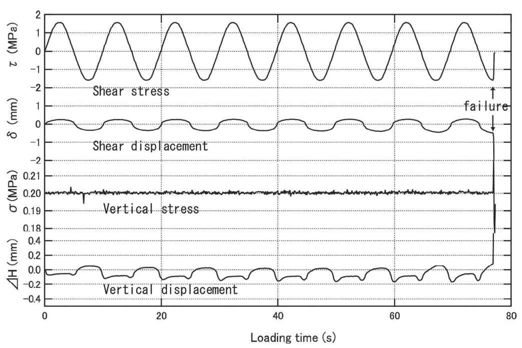

Figure 5. Example of result of fatigue test.

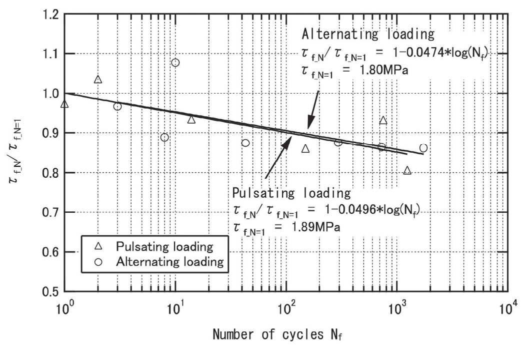

Figure 6. Cyclic test results.

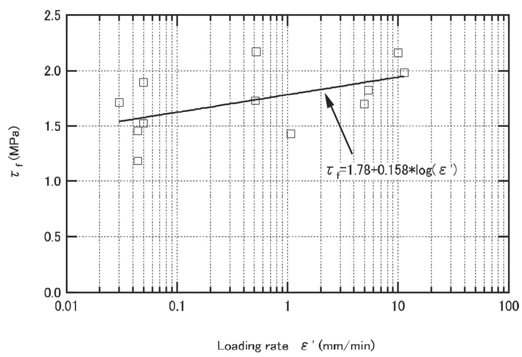

Figure 7. Relationship between loading rate and strength.

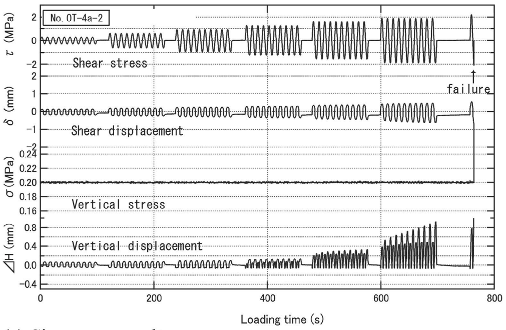

(a) Sine wave results

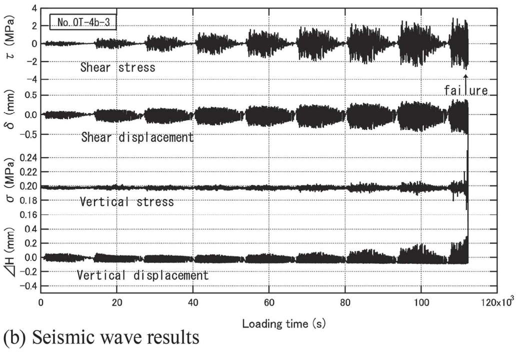

(b) Seismic wave results

Figure 8. Examples of multistep cyclic loading tests.

strength (i.e., the dynamic strength). In alternating loading, it appeared to be random whether failure occurred with shear stress τ on the positive or negative side.

The dynamic strength was obtained from the multistep cyclic test and then compared with the calculation result obtained by the evaluation formula. The static strength is set to the strength of $\sigma_f = 0.2$ MPa, as shown in Fig. 5. The calculation of the dynamic strength loading rate using the mathematical model proceeds in the following manner. Letting the loading time be the time required for N = 1/4 of a wave corresponding to the monotonic loading test from sine wave frequency f_r, the shear displacement at the time of fracture can be considered an almost constant value (0.65 mm) regardless of the loading rate, and converted to a displacement rate under conditions where failure displacement is reached at one amplitude. At this time, the displacement rate for $f_r = 0.1$ Hz is calculated as $\dot{\varepsilon} = 15.6$ mm/min. Under the present conditions where the shear stress increases at the same frequency in multiple steps, the smaller the stress amplitude, the smaller the displacement rate of the load. Therefore, when the stress amplitude is 1/5 relative to the static strength, the displacement rate is also calculated as 1/5.

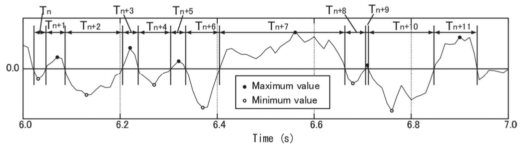

Figure 9. Illustration of frequency and stress history in a seismic wave.

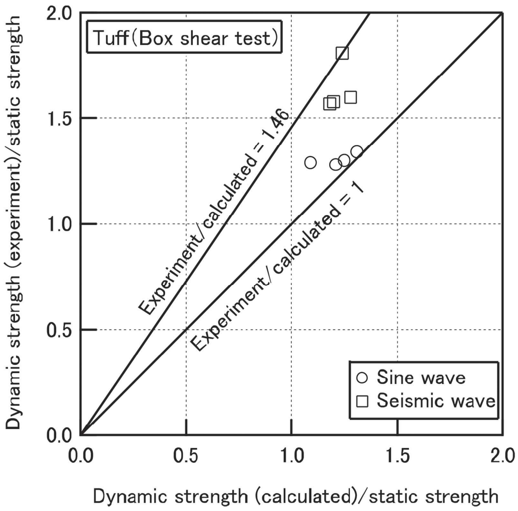

Figure 10. Comparison between experimental and calculated results.

The calculation of the seismic wave loading rate using the mathematical model proceeds in the following manner (Figure 9). The point where the seismic wave crosses the X axis (Y = 0) is identified, and the time interval (T_n) is obtained for each half wave. In the same way as for the sine wave, the shear displacement at the time of fracture rate was calculated as $\dot{\varepsilon} = 0.65/(T_n/2/60)$ mm/min. If the seismic wave time axis is stretched by 10 times, the displacement rate will be 1/10. In addition, as shown in Fig. 9, letting the respective stress histories be the maximum value on the positive side of the divided wave and the minimum value on the negative side, the dynamic strength is calculated separately for each side from the mathematical model, and the side with the maximum absolute value is taken as the dynamic strength.

Figure 10 shows the relationship between the dynamic strength obtained from the calculation and the dynamic strength obtained from the experiment normalized with the static strength. On the vertical axis, dynamic strength (experiment)/static strength is from 1.28 to 1.81. On the horizontal axis, the dynamic strength (calculated)/static strength is from 1.09 to 1.31. The seismic wave test tends to underestimate the result values in the mathematical model compared to the sine wave test. Comparing the experimental and calculated results, the experimental results were always 3–46% larger than the calculation results. In cases where the increase in the rate of the dynamic strength was relatively large in the experimental results, the calculation results also exhibit a relatively large strength result. This suggests that the mathematical model is generally reasonable.

Our assumption of the cumulative damage rule could explain why the seismic wave results underestimate the calculation results compared to sine waves, and why the calculation results always underestimate the experimental results. The cumulative damage rule is based on the assumption that internal damage accumulates linearly as the load increases. However, the relationship is thought to be nonlinear (the internal damage increases as the load increases).

In any case, because no experimental data is available, further research is needed. However, the fact that the strength of the experiment result is always larger than the calculation result can also be viewed as an advantage of our dynamic strength evaluation method, in the sense that it tends to err on the side of safety.

4 CONCLUSION

1. To clarify the impact of the alternating loading condition, which reverses the direction of the shear stress, a cyclic loading test was conducted on natural tuff. The results showed no difference in strength due to the loading condition (pulsating loading vs. alternating loading). Furthermore, similar to the previous studies, the dynamic strength was found to exceed the static strength during multistep loading under the alternating condition.
2. To clarify the relationship between the strength exerted under regular waves and irregular waves, the parameters required by the mathematical model were acquired, and a multistep cyclic loading test was performed using regular waves and irregular waves. These experimental results were then compared with the calculation results obtained from the mathematical model. The dynamic strength calculated using the mathematical model was slightly smaller than the dynamic strength obtained from the experiment. However, the results generally indicate that it is possible to evaluate the variation in the strength exerted owing to regular waves and irregular waves. Our results therefore demonstrate that it is possible to perform dynamic strength evaluation that errs on the side of safety based on a series of laboratory tests to acquire the parameters followed by the calculations in our model.

REFERENCES

Japan Electric Association. 2008. Nuclear Power Plant Seismic Design Guidelines, pp.155 (in Japanese).

Japanese Geotechnical Society. 2009. Method for direct shear test on a rock discontinuity, Geotechnical materials test methods and commentary, pp. 912–944.

Nishi, K. & Esashi, Y.1982. Study on the mechanical properties of mudstone (Part 4), Central Research Institute of Electric Power Industry Research Report 382014(in Japanese).

Nuclear power civil engineering committee ground stability evaluation subcommittee, 2004. J. of the Japan Society of Civil Engineers No. 757/III -66, pp. 21–31 (in Japanese).

Okada, T. & Ito, H. 2009. Mathematical modeling of the dynamic strength of soft rock, Proceedings of the 38th Symposium on Rock Mechanics(in Japanese).

Okuma, N., Eto, Y., Hatamoto, H., Joshita, M., Okawa, T. & Okada, T. 2010. Dynamic strength in cyclic 3-axis tests with different loading patterns using fault simulated specimens, Papers from the 39th symposium on rock dynamics (in Japanese).

Otaki, H. 2007. Mechanical fatigue strength design method, Nikkan Kogyo Shimbun(in Japanese).

Sugiyama, H, Saotome, A. & Nakamura, Y. 2001. Dynamic strength characteristics of volcanic breccia based on triaxial compression test, The 56th Annual Scientific Lecture Meeting of the Japan Society of Civil Engineers, pp. 134–135(in Japanese).

Tani, K. 2006. Shear strength of Oya tuff stone evaluated by in-situ triaxial test in the bedrock: Role and materials, Vol.55, No.5, pp. 483–488 (in Japanese).

Yoshinaka, R., Ogino, I., Takada, S. & Kanazawa, K.1987. Strength characteristics of sedimentary soft rock under dynamic cyclic loading, 7th National Symp. on Rock Mechanics in Japan technical papers, pp. 61–66(in Japanese).